THE JOURNAL OF COMPARATIVE NEUROLOGY 501:303–315 (2007)

Breathing and Calling: Neuronal Networks in the *Xenopus laevis* Hindbrain

ERIK ZORNIK* **AND DARCY B. KELLEY**
Department of Biological Sciences, Columbia University, New York, New York 10027

ABSTRACT

Xenopus laevis is an aquatic anuran with a complex vocal repertoire. Unlike terrestrial frogs, vocalizations are independent of respiration, and a single muscle group—the laryngeal dilators—produces underwater calls. We sought to identify the premotor neural network that underlies vocal behaviors. Vocal patterns generated by premotor networks control laryngeal motor neurons in cranial nucleus (n.) IX-X. Glottal motor neurons, active during respiration, are also present in n.IX-X. We used horseradish peroxidase (HRP), Lucifer yellow, and fluorescently conjugated dextrans to characterize the organization of n.IX-X and to trace premotor neuron projections. Premotor nuclei include the inferior reticular formation (Ri) adjacent to n.IX-X and the pretrigeminal nucleus of the dorsal tegmental area of the medulla (DTAM), the primary descending input to n.IX-X. Intramuscular HRP injections revealed a spatially segregated pattern, with glottal motor neurons in anterior n.IX-X and laryngeal motor neurons in the caudal portion of the nucleus. Dextran injections identified commissural n.IX-X neurons that project to the contralateral motor nucleus and DTAM-projecting n.IX-X neurons. Both neuronal types are clustered in anteromedial n.IX-X, closely associated with glottal motor neurons. Ri neurons project to ipsilateral and contralateral DTAM. Projections from DTAM target n.IX-X bilaterally, and all four identified subtypes receive DTAM input. In contrast, Ri neurons receive little input from DTAM. We hypothesize that connectivity between neurons in n.IX-X, Ri and DTAM may provide mechanisms to generate laryngeal and glottal activity patterns and that DTAM may coordinate vocal and respiratory motor pools, perhaps acting to switch between these two mutually exclusive behaviors. J. Comp. Neurol. 501:303–315, 2007.

Indexing terms: song; vocalization; respiration; isolated brain; hindbrain

The frog *Xenopus laevis* relies on underwater vocal signaling to coordinate courtship and male–male dominance behaviors (Wetzel and Kelley, 1983; Tobias et al., 2004). The adoption of an entirely aquatic lifestyle led to a novel mechanism of vocal production. In contrast to terrestrial frog calls (Martin and Gans, 1972), *Xenopus* calls are independent of respiration and use only a single set of muscles (Yager, 1992). This simplification makes *Xenopus* an excellent organism for studying vocal pattern generation and for investigating the evolutionary reconfiguration of terrestrial circuits to produce calls without breathing. The vocal repertoire consists of eight call types distinguishable by their temporal patterns (Tobias et al., 1998, 2004). These patterns are generated within the CNS (Yamaguchi and Kelley, 2000). Although candidate vocal nuclei have been identified in terrestrial and aquatic frogs, specific premotor vocal neurons and their connections have not been described in detail. We therefore sought to identify the underlying neural subtypes involved in the vocal hindbrain network.

The axons that make up the laryngeal motor nerve exit the brain via the most posterior root of cranial nerve (N.) IX-X (Simpson et al., 1986). These axons innervate intrinsic laryngeal muscles that produce calls and glottal muscles that are active during respiration. The laryngeal mo-

Grant sponsor: National Institutes of Health; Grant number: NS23684 (to D.B.K.); Grant sponsor: National Research Service Award; Grant number: DC6743-2 (to E.Z.).

*Correspondence to: Erik Zornik, MC 2430, Department of Biological Sciences, Columbia University, New York, NY 10027.
E-mail: ejz4@columbia.edu

Received 28 April 2006; Revised 24 June 2006; Accepted 19 July 2006
DOI 10.1002/cne.21145
Published online in Wiley InterScience (www.interscience.wiley.com).

tor nucleus (n.IX-X) contains vocal motor neurons, glottal motor neurons and interneurons (Kelley, 1980; Wetzel et al., 1985; Brahic and Kelley, 2003). Some interneurons project to contralateral n.IX-X and some to the major afferent to n.IX-X, the pretrigeminal nucleus of the dorsal tegmental area of the medulla, or DTAM (a rostral hindbrain nucleus). Medial to n.IX-X is the inferior reticular formation (Ri). Neurons in Ri may also project to DTAM. Direct synaptic connections between Ri and n.IX-X have not been established, but the dendrites of n.IX-X motor neurons extend into Ri (Kelley et al., 1988). These neuronal populations (see Fig. 1A) make up a candidate vocal premotor hindbrain network.

The aim of this study was to develop a fine-resolution map of neuronal subpopulations within hindbrain vocal nuclei. We defined neuronal subtypes based on their intranuclear locations, projection targets, and synaptic inputs through the use of anatomical tracers—horseradish peroxidase (HRP), Lucifer yellow (LY), and fluorescent dextran amines—alone or in combination. Some tracing experiments were performed in concert with axon bundle transections to determine axon trajectories. Results reveal candidate *X. laevis* hindbrain circuits for generating and coordinating temporally distinct vocal and respiratory motor patterns.

MATERIALS AND METHODS

Animals and overview of approaches

Sexually mature male *Xenopus laevis* were obtained from Xenopus One (Ann Arbor, MI) and Nasco (Fort Atkinson, WI). Animal care procedures adhered to NIH and Columbia University's Institutional Animal Care and Use Committee guidelines (protocol No. AAAA5759). In vivo injections of HRP into laryngeal dilator and glottal muscles allowed us to localize their motor pools in n.IX-X. To map neural populations and projections in the vocal circuit, anatomical tracers were applied in an isolated brain preparation (based on Luksch et al., 1996; modified by Brahic and Kelley, 2003, and in the current study; see details below). This in vitro preparation has been shown to retain morphological and physiological integrity for up to 5 days. Brains were examined in sections to observe cellular and axonal details or as whole mounts (as per Brahic and Kelley, 2003; described below), which allowed us to view cell populations and axon projections in their entirety. Each experiment was replicated in two to six additional animals.

HRP labeling of motor neurons in vivo

Animals were anesthetized [1.3% ethyl 3-aminobenzoate methanesulfonate salt (MS-222); Sigma, St, Louis, MO; 1.0 ml injected into the dorsal lymph sac] and placed on ice, and HRP crystals (Sigma; type VI, P-8375) were inserted into the exposed glottal and laryngeal muscles with insect pins. The larynx can be easily accessed via the mouth. The glottal muscles were exposed via a small incision just lateral to the glottal opening. The same approach was used to inject the laryngeal muscle on the other side of the larynx; a slightly larger incision was made about 1 cm posterior to the glottis, and the overlying tissue was removed to expose the laryngeal muscle. Multiple insertion sites covered the anterior-posterior extent of the muscle. Animals were allowed to survive for 3 days, after which they were anesthetized and perfused as described below. Brains were removed and fixed in 1.25% glutaraldehyde at 4°C overnight, equilibrated in 20% sucrose, cryosectioned, and processed with a tungstate-stabilized tetramethylbenzidine reaction (Weinberg and van Eyck, 1991) to reveal HRP activity in motor neurons.

In vitro brain preparation

Deeply anesthetized animals (MS-222) were placed on ice and transcardially perfused with 30 ml ice-cold oxygenated saline [75 mM NaCl, 25 mM $NaHCO_3$, 2 mM $CaCl_2$, 2 mM KCl, 0.5 mM $MgCl_2$, 11 mM glucose, oxygenated with carbogen (95% O_2, 5% CO_2) to a pH of 7.3, from Luksch et al. (1996); or a modified saline: 96 mM NaCl, 20 mM $NaHCO_3$, 2 mM $CaCl_2$, 2 mM KCl, 0.5 mM $MgCl_2$, 10 mM HEPES, 11 mM glucose, oxygenated with 99% O_2, 1% CO_2 to a pH of 7.5–7.7]. After perfusion, the spinal cord was transected below the brachial nerves, the brain was dissected in freshly oxygenated saline, and tracer was applied. We used three fluorescently labeled dextrans: fluoro-ruby (FR), fluoro-emerald (FE), and Cascade blue (CB; tetramethylrhodamine-, fluorescein-, and CB-conjugated dextran, respectively; anionic, lysine-fixable, 3,000 molecular weight; Molecular Probes, Eugene, OR; D-3308, D-3306, and D-7132). After transport, labeling is both anterograde (terminal fields) and retrograde (cell bodies). Motor neurons in n.IX-X were visualized via LY back-labeling of the fourth root of cranial nerve IX-X (see description below). After tracer application, brains were placed in ~500 ml of oxygenated saline and maintained at 4°C. We found that a large volume (500-750 ml) of oxygenated saline, changed daily, was sufficient to maintain brain tissue in good condition, without the need for constant oxygenation.

DTAM and n.IX-X injections

For n.IX-X injections, dextran tracers were applied via dye-coated minuten pins (Fine Science Tools, no. 26002-10). n.IX-X begins just anterior to the insertion site of the caudal root of N.IX-X and extends caudally ~1 mm, just posterior to the obex. Neurons in the nucleus are arranged in a column (~0.2 mm diameter) along this axis, with the lateral edge of the nucleus ~0.25 mm from the lateral surface of the brain. From a lateral approach, FR pins were inserted 0.4–0.5 mm below the brain surface along this column by using the nerve and obex as markers. A similar method was employed for double-label experiments, in which FR was injected into anterior and FE into posterior n.IX-X. In these injections, care was taken to ensure that injection sites did not overlap such that the "injection column" of each dye was slightly less than 0.5 mm in length.

For DTAM, FR was applied via pin application (as above) or by pressure injection as a 15% solution in saline, front-loaded into a borosilicate glass capillary tube (1.0 mm OD and 0.75 mm ID/fiber; FHC, Bowdoinham, ME; No. 30-30-0) drawn on a microelectrode puller (Sutter Instrument Co., Novarto, CA; model P-87), then broken back to a 20–24-μm tip. The saline level was lowered, and the pipette tip was placed into DTAM. DTAM can be reproducibly located by using external landmarks; it lies just lateral to the fourth ventricle edge and is immediately posterior to the optic tectum-cerebellum border about 1.5 mm below the surface of the cerebellum. Dye was administered with 4–10 pressure pulses (20 psi, 20 msec; Pico-

spritzer II; General Valve Corporation), such that the majority of the nucleus (an ~300-μm-diameter sphere) was infused with dye.

Laryngeal nerve backfills

Brains were dissected as described above, with ~0.5 cm of the laryngeal nerve left intact, pinned onto saline-filled Sylgard dishes, and appropriate tracers were applied to DTAM and/or n.IX-X. Vaseline wells were then formed around the nerves, which were filled with 4% LY (Sigma; L0259) in 100 mM LiCl. With the saline constantly oxygenated, the Sylgard dishes were maintained overnight at 4°C. The nerve was then detached from the well and the brain moved to a larger container of fresh saline, which was changed daily until fixation.

Histology and photomicrography

After a 1–4-day survival, brains were fixed overnight in 4% paraformaldehyde in 0.1 M phosphate buffer (pH 7.3; Sigma). For sections, brains were equilibrated in 20% sucrose, sectioned in the horizontal or transverse plane at 30 μm on a cryostat (Hacker Instrument Company), serially dehydrated in ethanol, cleared in xylene, and coverslipped. For whole mounts, meninges were removed from the fixed brain tissue, which was subsequently dehydrated in increasing concentrations of ethanol, and cleared in methyl salicylate.

Brain sections and whole mounts were observed with epifluorescent or brightfield illumination on a Leica DMR microscope, and photomicrographs were taken using a Spot digital camera (Diagnostic Instruments, Sterling Heights, MI; software version 4.0.4). Whole mounts were viewed in a depression slide immersed in methyl salicylate. Images were prepared in Adobe Photoshop; the Levels and Brightness/Contrast functions were used to highlight tissue outlines and optimize visualization of cellular detail. Uneven illumination of brightfield images was corrected with the Dodge tool (variable radius; exposure 10–15%).

RESULTS

Glottal and laryngeal motor neurons in n.IX-X

Nissl-stained horizontal sections at the level of n.IX-X reveal neurons clustered in a rostrocaudal column (~0.2 mm diameter), which begins just anterior to the nerve insertion point and extends caudally for ~1 mm (Fig. 1B, right). Motor neurons in n.IX-X can be identified by backlabeling the fourth root of N.IX-X with LY (Fig. 1B, left). These neurons include both laryngeal and glottal motor neurons. To determine the spatial relation between these two cell types, we compared the locations of labeled cell bodies following HRP injections into glottal and laryngeal muscles (Fig. 1C). In each animal, HRP was injected into the left glottal muscle and into the right laryngeal muscle. These experiments revealed that glottal and laryngeal motor neurons are spatially segregated (Fig. 1C, right); glottal motor neurons occupy the anterior extent of n.IX-X, whereas laryngeal dilator motor neurons are found in the posterior portion of the nucleus.

In some sections, a few labeled cells in anterior n.IX-X were present on the side of laryngeal dilator muscle injection (Fig. 1C, asterisk). These probably are due to HRP uptake by glottal motor neuron axons, which enter the dilator muscle caudally and travel anteriorly until reaching the glottal muscle. Smaller numbers of back-labeled motor neurons on the side of glottal muscle injections were observed in posterior n.IX-X (Fig. 1C, arrow). These few cells are likely the result of HRP diffusion out of the injection site and into the laryngeal muscle resulting from the relatively small size of the glottal muscles.

Projection neurons in n.IX-X and Ri

Commissural neurons. Fluoro-ruby (FR) injected into n.IX-X revealed retrogradely labeled cells—IX-$X_{IX\text{-}X}$ neurons—in the contralateral motor nucleus and in Ri. Relatively small neurons in Ri were found throughout the nucleus (Fig. 2A,B). Larger IX-$X_{IX\text{-}X}$ neurons were concentrated in the anteromedial region of the nucleus (Fig. 2A,B).

Do commissural neurons project throughout the contralateral motor nucleus or instead specifically target the anteromedial zone? Injections of red FR and green FE dextran amines into anterior and posterior n.IX-X, respectively, revealed both red and green singly labeled commissural neurons interspersed in the contralateral nucleus (Fig. 2C). Thus, commissural neurons project to either anterior (glottal) or posterior (laryngeal) zones of the n. IX-X motor nucleus, but different projection types are not segregated. We observed very few double-labeled commissural neurons, suggesting that contralateral input to glottal and laryngeal portions of n.IX-X is not shared.

In this experiment, cells in Ri were also retrogradely labeled, red cells in anterior Ri and green cells in posterior Ri (data not shown). In contrast to IX-$X_{IX\text{-}X}$ neurons, commissural neurons in Ri may be topographically segregated: anterior Ri commissural neurons send axons to either anterior n.IX-X or anterior Ri, and posterior Ri commissural neurons send axons to either posterior n.IX-X or posterior Ri.

DTAM-projecting neurons. Retrogradely labeled neurons were present in ipsilateral n.IX-X after FR injections into DTAM (Fig. 3A), confirming previous results (Wetzel et al., 1985; Brahic and Kelley, 2003). These labeled DTAM-projecting neurons (IX-X_{DTAM}) were present throughout ipsilateral n.IX-X but clustered in the anteromedial region (Fig. 3A). A few labeled cells were also found in contralateral n.IX-X (IX-X_{cDTAM}; not shown). A sparse pattern of retrogradely labeled neurons was observed in ipsilateral and contralateral Ri (data not shown). We conclude that most DTAM-projecting neurons in n.IX-X are ipsilateral and located in the anteromedial aspect of the nucleus.

What is the topographic relation of IX-X_{DTAM} and IX-$X_{IX\text{-}X}$ neurons? The results of triple-label experiments reveal that, within anterior n.IX-X, both types are interspersed with motor neurons (Fig. 3B). This triple-label protocol revealed a small number of doubly labeled interneurons in n.IX-X ipsilateral to the DTAM injection (Fig. 3B, inset). Thus, some n.IX-X projection neurons may target both DTAM and contralateral n.IX-X. Another possibility is that individual n.IX-X neurons simultaneously project to both ipsilateral and contralateral DTAM nuclei, where the contralateral axon passes through, or near, the n.IX-X injection site. To determine whether label via fibers of passage contributed to the observation of double-labeled cells, we injected each DTAM nucleus with a different colored dextran. We never observed double-labeled neurons in either n.IX-X or Ri under these conditions. We thus

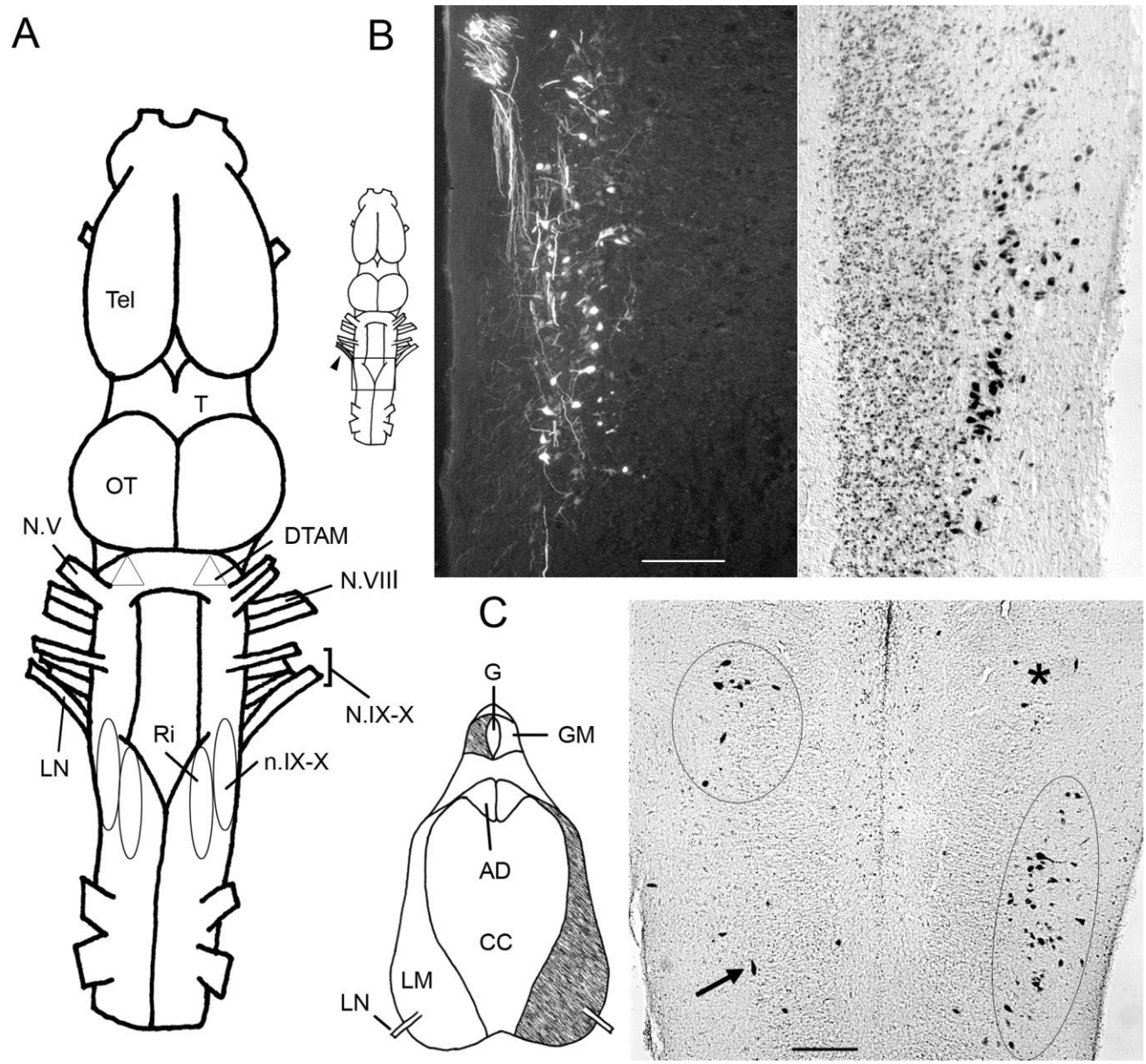

Fig. 1. Organization of cranial motor nucleus (n.) IX-X. **A:** Dorsal view of the *Xenopus laevis* brain. Anterior is up in all panels. Relevant hindbrain nuclei are indicated. **B:** Diagram: Laryngeal nerve (LN) shaded (arrowhead). Rectangle indicates area represented in adjacent photomicrographs. Left: Motor neurons in n.IX-X after Lucifer yellow (LY) backfill. Right: Contralateral horizontal section stained with cresyl violet. **C:** Dorsal view of the larynx. Shaded areas indicate location of horseradish peroxidase (HRP) injection: left glottal muscle and right laryngeal dilator. Adjacent photomicrograph of horizontal section: HRP-labeled glottal motor neurons (left oval, anterior) and laryngeal motor neurons (right oval, posterior). Asterisk and arrow indicate a few spuriously labeled cells (see Results). Tel, telencephalon; T, thalamus; OT, optic tectum; DTAM, pretrigeminal nucleus of the dorsal tegmental area of the medulla; N.V, trigeminal nerve; N.VIII, auditory nerve; N.IX-X, glossopharyngeal-vagal nerve; n.IX-X, laryngeal-glottal motor nucleus; Ri, inferior reticular formation; LN, laryngeal nerve; G, glottis; GM, glottal muscle; AD, arytenoid disc; CC, cricoid cartilage; LM, laryngeal muscle. Scale bars = 250 μm.

conclude that n.IX-X contains a third population of interneurons: those projecting both to DTAM and to contralateral n.IX-X.

Summary. Nucleus IX-X contains five neuron types. Glottal motor neurons are present in anterior n.IX-X, and there are laryngeal motor neurons in the posterior pole. Two major interneuron types, IX-$X_{IX\text{-}X}$ and IX-X_{DTAM}, are concentrated in anterior n.IX-X. A third, less prominent interneuron type projects to both DTAM and contralateral n.IX-X.

Commissural neuron projections to n.IX-X and Ri

In addition to identifying neuron subtypes within n.IX-X, we also wished to describe projections to the motor nucleus. After FR injections into n.IX-X, anterograde pro-

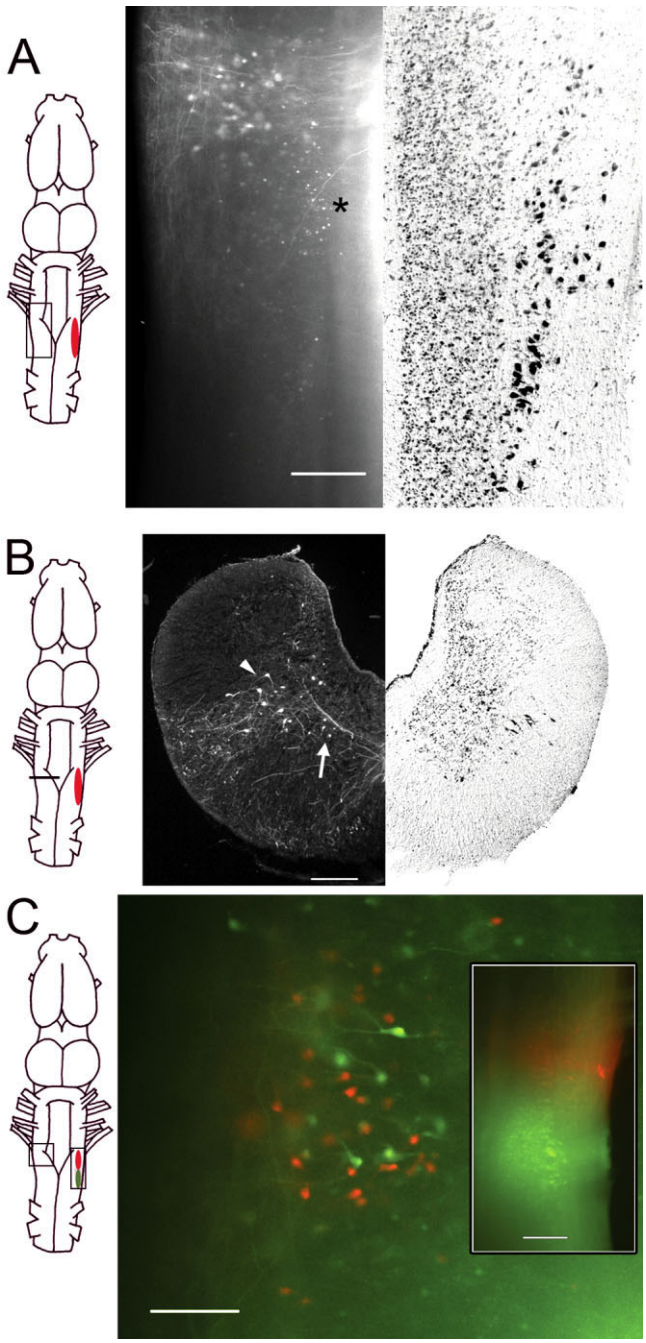

Fig. 2. Commissural interneurons: n.IX-X injections. **A:** Fluoro-ruby (FR) injection into n.IX-X. Photomicrograph of a whole-mount brain showing commissural interneurons (IX-X_{IX-X}) labeled in antero-medial contralateral n.IX-X [left; compare with adjacent cresyl violet-stained horizontal section (right)]. Asterisk indicates labeled neurons in contralateral Ri. **B:** Photomicrograph of n.IX-X commissural neurons in a transverse section. Dorsal is up. Arrowhead points to large IX-X_{IX-X} neurons; arrow shows smaller neurons in Ri. **C:** Nucleus IX-X labeled cells after injection of FR and fluoro-emerald (FE) into anterior and posterior, respectively, contralateral n.IX-X. Labeled IX-X_{IX-X} neurons are clustered in anterior n.IX-X (as in A), but red and green neurons are interspersed. The brain is viewed in whole mount. **Inset:**FR and FE injection sites into contralateral n.IX-X. Anterior is up. Scale bars = 250 μm in A,B,inset; 200 μm in C.

jections filled the entire contralateral nucleus with dense and uniform terminal fields (Fig. 4B; these terminals cannot be easily discerned in whole mounts and are therefore not visible in Fig. 2A). Terminals were also present throughout Ri (Fig. 4C). However, the density of these projections was considerably less than that seen in n.IX-X. Thus, IX-X_{IX-X} neurons preferentially target contralateral n.IX-X as opposed to contralateral Ri.

To what neuron type do commissural neurons project? Backfills of the laryngeal nerve with LY were combined with FR injections into contralateral n.IX-X (Fig. 5A, diagram). In these experiments, anterogradely filled axon terminals with bouton-like structures were observed in close proximity to labeled cell bodies and dendrites of motor neurons throughout n.IX-X (Fig. 5A). The most likely interpretation of this finding is that n.IX-X motor neurons (both glottal and laryngeal dilator) receive direct input from IX-X_{IX-X} neurons.

After FR injection into n.IX-X, retrogradely labeled neurons did not appear to be contacted by anterogradely labeled terminals (not shown). Thus, IX-X_{IX-X} neurons do not make conspicuous reciprocal contacts with their contralateral counterparts. Double injections (Fig. 5B; FR in DTAM, FE in contralateral n.IX-X) were used to assess whether DTAM-projecting neurons receive input from commissural neurons. In the motor nucleus ipsilateral to the DTAM injection site, green terminals from contralaterally projecting neurons cover the somata and proximal dendrites of IX-X_{DTAM} neurons (Fig. 5B, right). We suggest, therefore, that IX-X_{DTAM} neurons receive synaptic input from contralateral n.IX-X.

DTAM projections to n.IX-X and Ri

Neurons in DTAM also project to n.IX-X ($DTAM_{IX-X}$ neurons). DTAM injections revealed anterogradely labeled axons in n.IX-X and dense terminal fields throughout the nucleus (Fig. 6B). In contrast, label in Ri was sparse along the anterior-posterior extent of n.IX-X (Fig. 6C). The same pattern, albeit with somewhat less labeling, was observed in contralateral n.IX-X. We conclude that $DTAM_{IX-X}$ neurons preferentially target n.IX-X rather than Ri.

Do neurons in DTAM project directly to motor neurons? To verify that DTAM targets motor neurons, DTAM was injected with FR, and the laryngeal nerve was backfilled with LY to label motor neurons. Motor neuron cell bodies were robustly decorated with terminals of axons arising from DTAM in both the anterior (Fig. 7A) and the posterior (Fig. 7B) extent of n.IX-X. Insofar as anterior n.IX-X contains glottal motor neurons and posterior n.IX-X contains laryngeal dilator motor neurons, these results reveal that DTAM neurons target both cell types.

Do $DTAM_{IX-X}$ neurons project to IX-X_{IX-X} and IX-X_{DTAM} neurons? DTAM was injected with FR, and the contralateral n.IX-X was injected with FE. Resulting sections showed green, retrogradely labeled IX-X_{IX-X} neurons decorated with red axon terminals (Fig. 7C). Single FR injections into DTAM also revealed anterogradely labeled DTAM fibers that decorate IX-X_{DTAM} neuron cell bodies (Fig. 7D). Examples of DTAM contacts with Ri neurons were not observed. We conclude that DTAM provides input to both commissural and DTAM-projecting neurons in n.IX-X. Thus, DTAM projects to four identified n.IX-X subtypes—glottal and laryngeal motor neurons, IX-X_{IX-X}

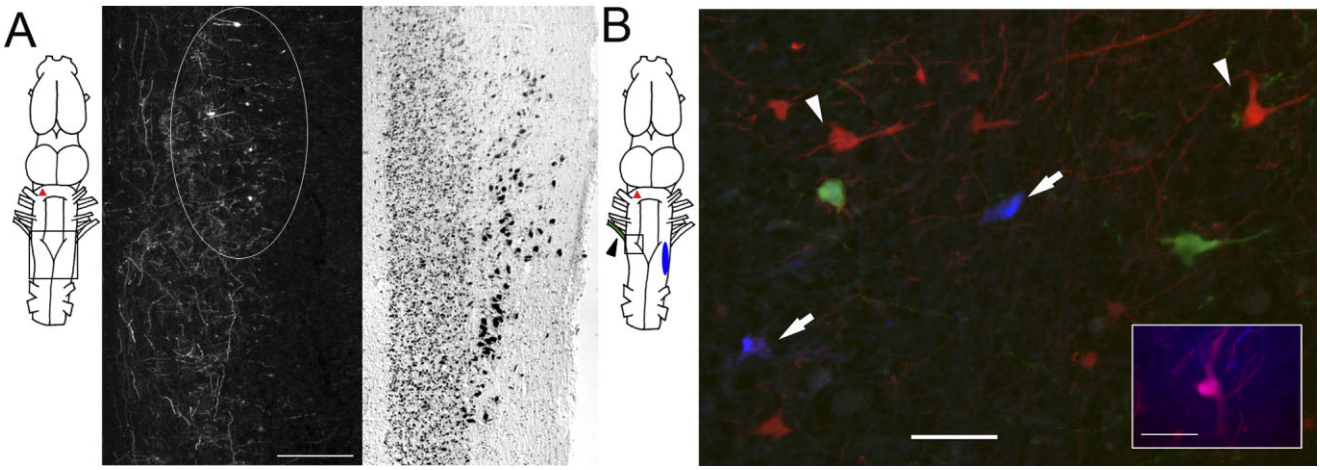

Fig. 3. DTAM-projecting neurons in n.IX-X: DTAM injections. **A:** DTAM-projecting neurons in n.IX-X ($IX\text{-}X_{DTAM}$) following FR injection into DTAM. Horizontal section; anterior is up. $IX\text{-}X_{DTAM}$ neurons are clustered in anteromedial n.IX-X (indicated by oval). **B:** Labeled neurons in n.IX-X following LY-backfilling of N.IX-X (green), FR injection into ipsilateral DTAM (red), and Cascade blue (CB) injection into contralateral n.IX-X (blue). $IX\text{-}X_{DTAM}$ neurons in n.IX-X (red; arrowheads) are interspersed with $IX\text{-}X_{IX\text{-}X}$ neurons (blue; arrows) and anterior motor neurons (green). **Inset:** Double-labeled (magenta) neuron in anterior n.IX-X. Scale bars = 250 μm in A; 50 μm in B,inset.

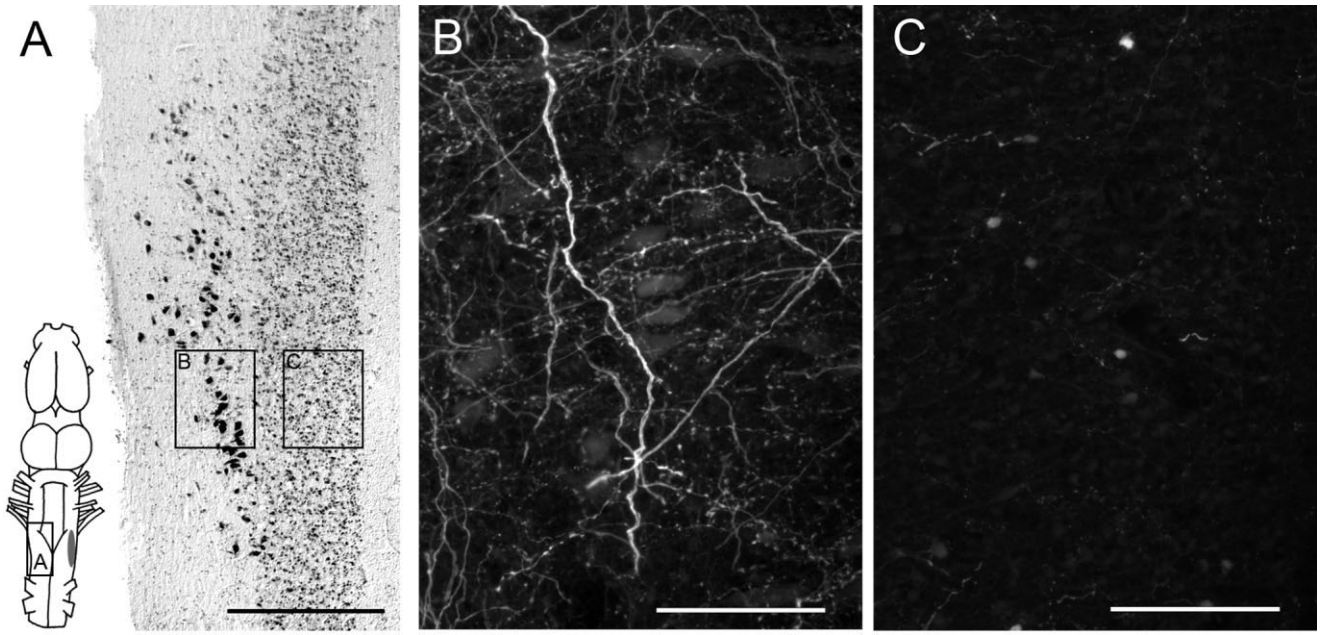

Fig. 4. Projections to contralateral n.IX-X and Ri: n.IX-X injections. **A:** Diagram: Shaded oval indicates FR injection into n.IX-X. Boxes: Regions of n.IX-X and Ri illustrated in A, B, and C. Photomicrograph: Horizontal section containing n.IX-X and Ri stained with cresyl violet. **B:** High-magnification view of n.IX-X showing axon fibers and terminals. **C:** Very sparse pattern of $IX\text{-}X_{IX\text{-}X}$ neuron fibers and terminals in Ri. Scale bars = 500 μm in A; 100 μm in B,C.

neurons, and $IX\text{-}X_{DTAM}$ neurons—underscoring the observation of a robust connection between these nuclei.

DTAM projection neurons

As demonstrated above, tracer injections into DTAM produce anterogradely labeled axon terminals in n.IX-X bilaterally. Injections of FR into n.IX-X retrogradely label the source of these projections, DTAM projection neurons ($DTAM_{IX\text{-}X}$), in ipsilateral and contralateral DTAM (Fig. 8A; see also Brahic and Kelley, 2003). Simultaneous injections of ipsilateral and contralateral motor nuclei (FE, ipsilateral; FR, contralateral) produce three classes of labeled cells in DTAM—ipsilaterally projecting (green), contralaterally projecting (red), and bilaterally projecting (yellow, double-labeled) neurons (Fig. 8B)—which appear to be evenly distributed throughout the nucleus. To determine whether subpopulations of $DTAM_{IX\text{-}X}$ neurons project specifically to either glottal or laryngeal zones in

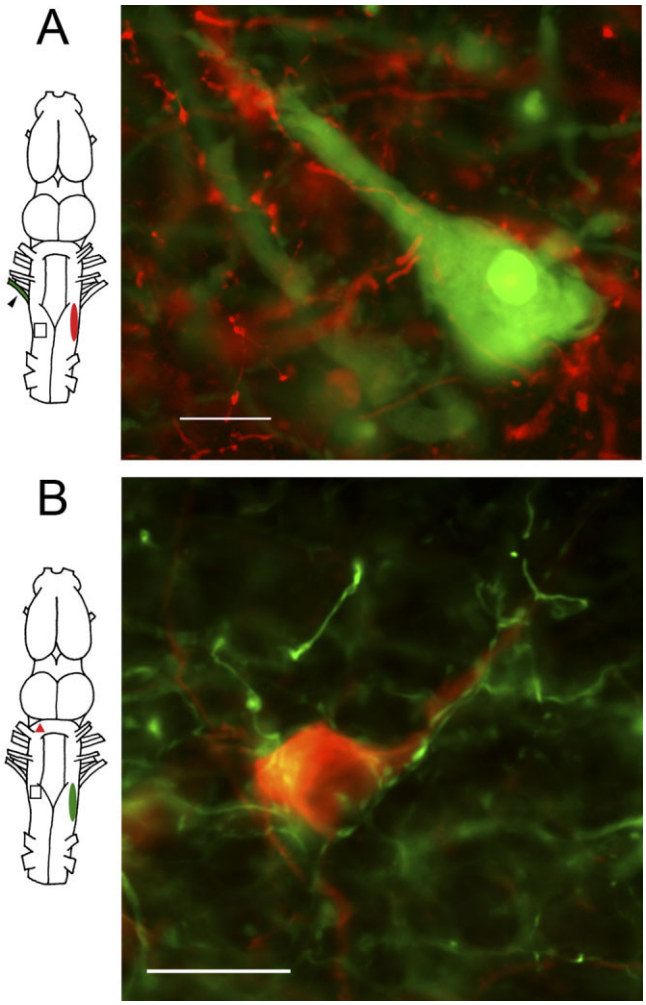

Fig. 5. Commissural neuron projection targets: n.IX-X injections. **A:** Axon terminals from IX-$X_{IX\text{-}X}$ neurons (red) in close proximity to soma and dendrites of LY-backfilled motor neurons (green) suggest possible synaptic inputs. **B:** Anterogradely labeled IX-$X_{IX\text{-}X}$ axon terminals (FE injection into n.IX-X) make contact with retrogradely labeled IX-X_{DTAM} neurons (FR injection into DTAM). Scale bars = 20 μm.

n.IX-X, we injected FR into anterior, and FE into posterior, n.IX-X. Results showed singly labeled red and green cells and doubly labeled yellow neurons interspersed throughout DTAM (not shown). Thus the topographic organization of motor neurons in n.IX-X (anterior: glottal; posterior: laryngeal; Fig. 1C) is not reflected in the locations of their major afferent source, DTAM.

Projections to DTAM

Do terminals from IX-X_{DTAM} neurons make direct contacts with $DTAM_{IX\text{-}X}$ neurons? After n.IX-X injection, terminal fields filled ipsilateral DTAM in its entirety (Fig. 8A,C). Cell bodies and dendrites of bilaterally projecting (Fig. 8C), contralaterally projecting (Fig. 8D), and ipsilaterally projecting (not shown) $DTAM_{IX\text{-}X}$ neurons were decorated with axon terminals from n.IX-X. Thus all three subtypes of $DTAM_{IX\text{-}X}$ neurons receive input from n.IX-X. Sparse axon terminals were also found in contralateral DTAM following injections into n.IX-X (not shown). These terminals were not robust enough to identify the cell types that they target. We conclude that all $DTAM_{IX\text{-}X}$ subtypes may receive input from ipsilateral n.IX-X. DTAM also receives inputs from contralateral n.IX-X, but the specific targets of these projections are unknown.

Axon trajectories

A common problem in these dye-tracing experiments is transport resulting from uptake by fibers of passage. DTAM neurons project to both ipsilateral and contralateral n.IX-X ($DTAM_{iIX\text{-}X}$ and $DTAM_{cIX\text{-}X}$, respectively). It is possible that axons from both neuron types first descend to the level of ipsilateral n.IX-X; some neurons synapse ipsilaterally, whereas others would cross the midline and then find their targets. If this is so, results illustrated in Figures 4 and 5 might represent terminals from $DTAM_{cIX\text{-}X}$ neurons rather than terminals from IX-$X_{IX\text{-}X}$ neurons. To resolve this issue, we followed axon trajectories in whole-mount brains after FR was injected into n.IX-X.

Two major commissural tracts, a caudal one at the level of n.IX-X and a rostral one at the level of DTAM, were present. We observed both ipsilaterally and contralaterally labeled neurons in DTAM following n.IX-X injection. Ipsilateral projections leave DTAM laterally, extending to a superficial axon tract, which turns caudally and ventrally to reach n.IX-X (Fig. 9A). Contralateral neurons could have been labeled due to transport via uptake from axons in the posterior commissure. However, when we repeated this experiment with a transection through the tract between n.IX-X and DTAM, the normal distribution of labeled cells in DTAM contralateral to the injection site was still present (Fig. 9B; transection illustrated). This result indicates that cells within DTAM that project to contralateral n.IX-X first cross the midline at the level of DTAM before descending to the opposite n.IX-X. These results are supported by our observations of the anterior commissure. At a focal plane just ventral to DTAM (Fig. 9C), fibers that will form the anterior commissure travel slightly ventral and anterior of DTAM to cross the midline, then join other DTAM fibers descending toward n.IX-X.

To identify the axon trajectories of neurons in n.IX-X or Ri that project to contralateral DTAM, we injected FR into DTAM in brains transected through the anterior or posterior commissure. In experiments with a posterior commissure transection, we did not observe retrogradely labeled neurons in either contralateral n.IX-X or Ri. However, labeled neurons were still found in this region after transections through the anterior commissure (data not shown). In other experiments, n.IX-X was injected, and transections were made through the anterior commissure or the contralateral tract that connects DTAM and n.IX-X. In these experiments also, robust terminals were found in contralateral n.IX-X, confirming that these terminals arise from contralaterally projecting IX-$X_{IX\text{-}X}$ neurons (as proposed in Fig. 4) and not retro- then anterogradely labeled bilaterally projecting $DTAM_{IX\text{-}X}$ neurons. Together, these results suggest that the posterior commissure is made up largely of the axons of IX-$X_{IX\text{-}X}$ neurons. The posterior commissure also contains axons from contralaterally projecting IX-X_{cDTAM} and Ri_{cDTAM} neurons.

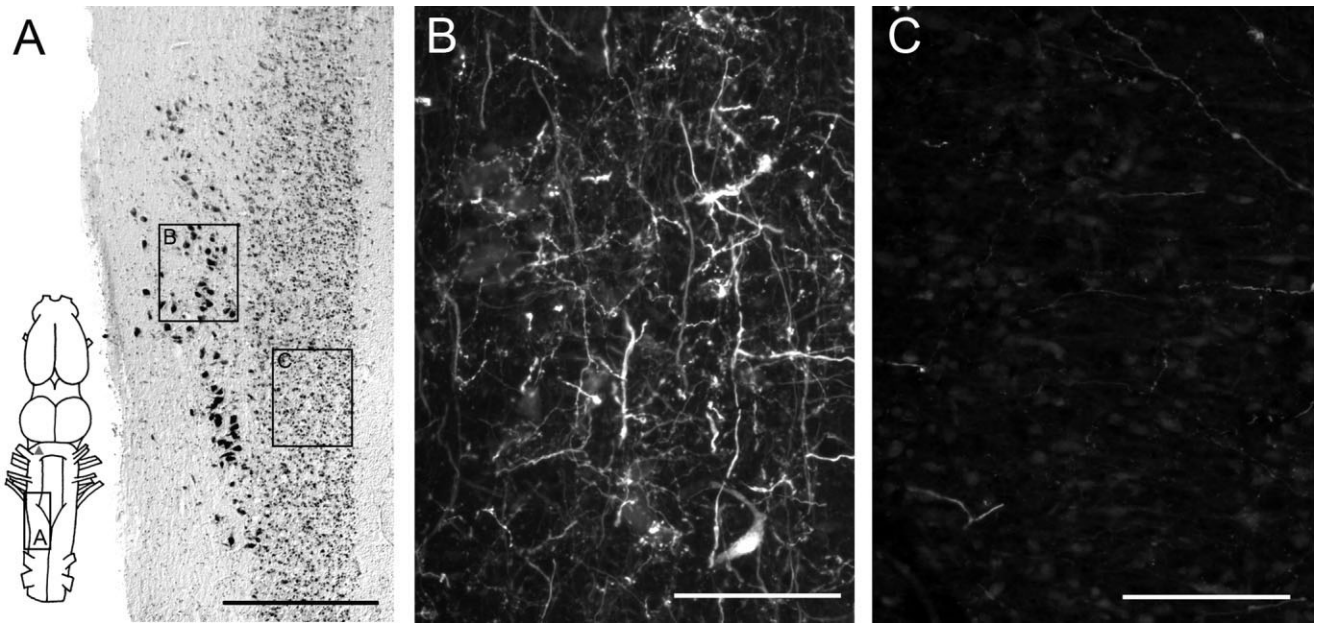

Fig. 6. DTAM projections to n.IX-X and Ri: DTAM injections. **A:** Diagram: Shaded triangle indicates FR injection into DTAM. Boxes: Regions of n.IX-X and Ri illustrated in A, B, and C. Photomicrograph: Horizontal section stained with cresyl violet containing n.IX-X and Ri. **B:** High-magnification view of n.IX-X with large number of axons, bouton-like structures, and one labeled neuron. **C:** Sparse pattern of axon fibers and terminals from DTAM neurons that project to n.IX-X ($DTAM_{IX-X}$). Representative of labeling throughout the anterior-posterior extent of Ri. Scale bars = 500 μm in A; 100 μm in B,C.

Contralateral inputs from the medial reticular formation

Injections into n.IX-X revealed several retrogradely labeled neurons in the contralateral anterior medulla within the medial reticular formation (Rm) anterior to Ri (Fig. 10A,B). Axons project contralaterally toward the lateral fiber tracts and then turn caudally to reach n.IX-X. Rm neurons are ventral and slightly caudal to DTAM (Fig. 10B) and, unlike DTAM neurons, project only to the contralateral motor nucleus.

DISCUSSION

Vocal networks in *X. laevis*: rationale and goals

Xenopus laevis males use their rich vocal repertoire during inter- and intrasexual communication. Relative to that in terrestrial vertebrates, the vocal production system in *Xenopus* is simplified. Calls are independent of breathing (Yager, 1992) and are produced by the contraction of a single set of muscles (Tobias and Kelley, 1987). These features—a rich vocal repertoire and simplified sound production—make *Xenopus* a powerful model system in which to study vocal pattern generation. *Xenopus laevis* belongs to the family Pipidae, aquatic anurans that diverged from terrestrial anurans ~150 million years ago (mya). Extant species of *Xenopus* originated ~50 mya (Evans et al., 2004) and, as with all other pipids, are completely aquatic. The vocal system of *Xenopus* thus also allows us to examine the neural underpinnings of the transition from a terrestrial environment, in which vocalization is closely tied to respiration, to an aquatic environment, in which sound production has been separated from breathing.

The temporal patterns of *Xenopus* songs reflect activity in a network of premotor and motor neurons in the hindbrain (Shaw and Kelley, 2005). Although basic connections of vocal hindbrain nuclei have been described, the identity and projections of specific neuron types in posterior (n.IX-X and Ri) and anterior (DTAM) hindbrain were not known. The development of the isolated brain preparation (Luksch et al., 1996; Brahic and Kelley, 2003) allowed us reproducibly to apply tracers and to perform double- and triple-label experiments with or without transections through fiber tracts. We used these multiple label preparations to identify vocal neuron subtypes and their projection targets. This study had two goals: 1) to establish a cell-type specific map of the hindbrain vocal network and 2) to describe anatomical relations between vocal and respiratory pathways.

Summary of results

The organization of premotor and motor vocal neuron types and their targets that we found is summarized in Figure 11. In the rostral hindbrain, DTAM projects bilaterally to n.IX-X and contains three types of projection neurons: ipsilateral, contralateral, and bilateral $DTAM_{IX-X}$ neurons (Fig. 11A). Each $DTAM_{IX-X}$ type receives input from ipsilateral n.IX-X via DTAM-projecting neurons ($IX\text{-}X_{DTAM}$; Fig. 11B). DTAM-projecting neurons in n.IX-X and Ri also project to contralateral DTAM (Fig. 11B). In the caudal hindbrain, n.IX-X is connected bilaterally. Commissural neurons located in anterior n.IX-X ($IX\text{-}X_{IX-X}$ neurons) project to

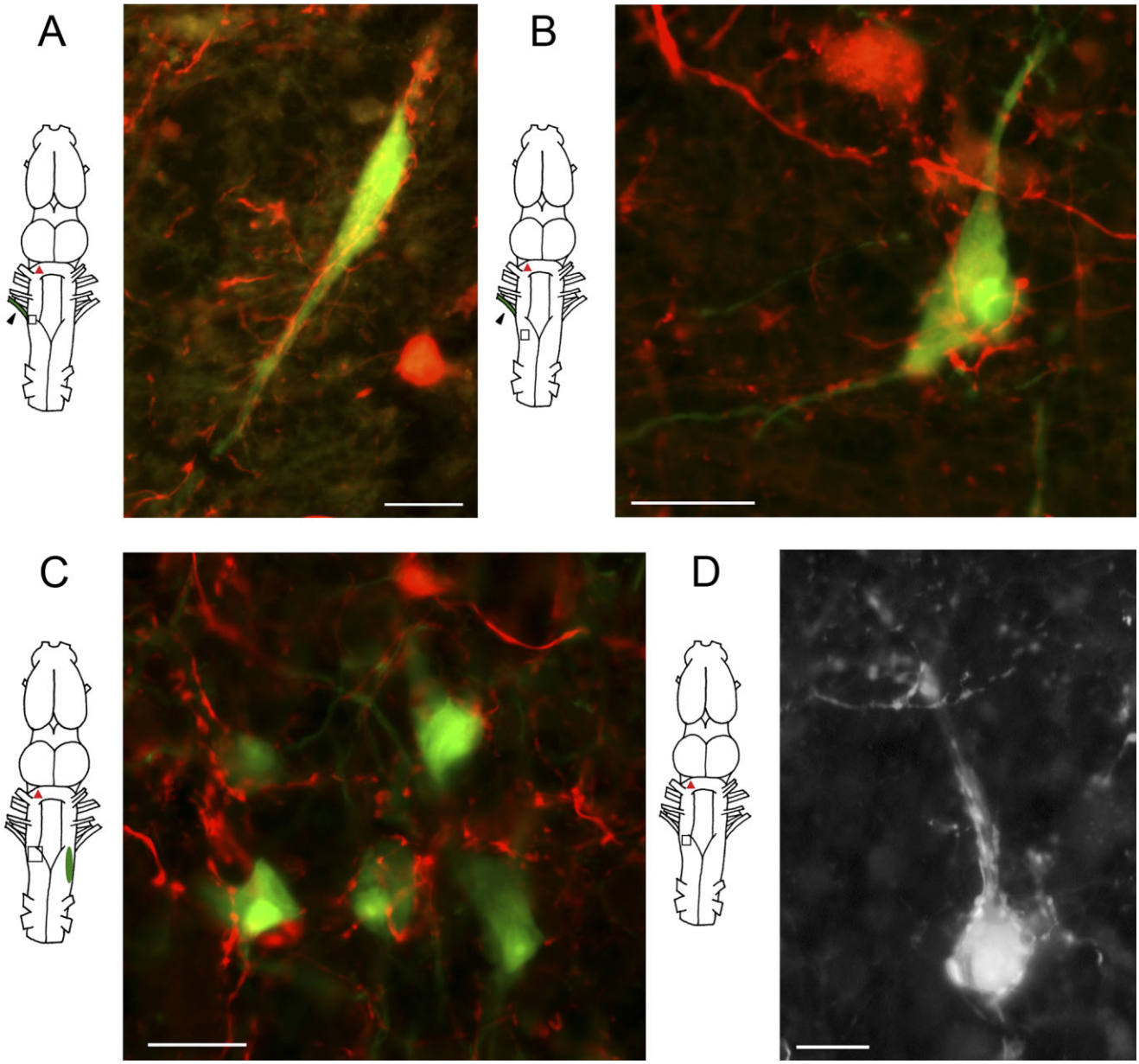

Fig. 7. DTAM projection targets in n.IX-X: DTAM injections. **A:** Axon terminals from DTAM provide extensive contacts onto LY-backfilled motor neuron in anterior n.IX-X. **B:** Similarly robust inputs from DTAM onto a posterior motor neuron. **C:** DTAM projection terminals in proximity to retrogradely labeled IX-$X_{IX\text{-}X}$ neurons. **D:** Retrogradely labeled IX-X_{DTAM} neuron also receives robust input from DTAM terminals. Scale bars = 20 μm in A–C; 10 μm in D.

anterior or posterior contralateral n.IX-X (Fig. 11C). Glottal and laryngeal motor neurons are spatially segregated; glottal motor neurons occupy anterior n.IX-X, whereas laryngeal motor neurons occupy posterior n.IX-X. IX-$X_{IX\text{-}X}$ neurons target at least three neuron types in contralateral n.IX-X: glottal motor neurons, laryngeal motor neurons, and DTAM-projecting neurons (Fig. 11C). Finally, neurons in DTAM make conspicuous contacts with four identified neuron types in n.IX-X: glottal motor neurons, laryngeal motor neurons, contralaterally projecting neurons, and DTAM-projecting neurons (Fig. 11D).

Role for DTAM in vocal production

Previous anatomical studies in *X. laevis* identified a reciprocal connection between DTAM and n.IX-X (Wetzel et al., 1985; Brahic and Kelley, 2003). In the present study, we have shown that this reciprocal connection is extremely robust. $DTAM_{IX\text{-}X}$ neurons project to four identified cell types in n.IX-X, and IX-X_{DTAM} neurons contact all three projection cell types in DTAM (Fig. 11B,D). This result strongly supports the hypothesis that DTAM is critical for vocal production.

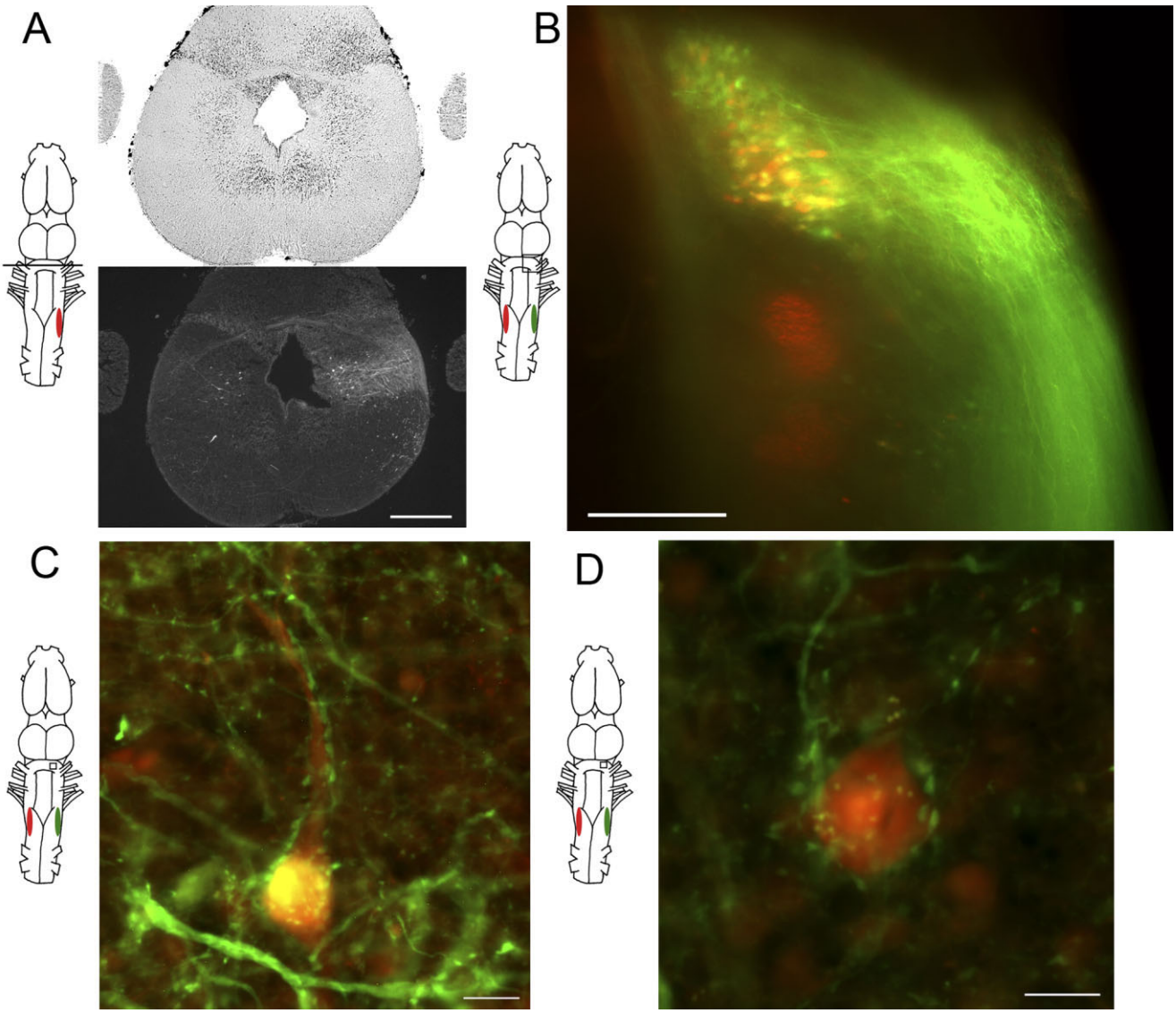

Fig. 8. DTAM neurons that project to n.IX-X and inputs to DTAM: n.IX-X injections. **A:** Transverse section shows $DTAM_{IX-X}$ neurons in ipsilateral and contralateral DTAM following FR injection into n.IX-X. Ipsilateral DTAM (right) receives robust anterograde input indicated by dense terminal fields. Contralateral DTAM (left) shows a very sparse pattern of axon terminals. Dorsal is up. **B:** DTAM in a whole-mount preparation following injections of FR and FE into left and right n.IX-X, respectively. Single-labeled cells project either ipsilaterally (green) or contralaterally (red). Double-labeled cells (yellow) project bilaterally. **C:** High-magnification photomicrograph (horizontal section) in DTAM reveals green terminals from ipsilateral n.IX-X contacting a bilaterally projecting $DTAM_{IX-X}$ neuron (yellow). **D:** A contralaterally projecting $DTAM_{IX-X}$ neuron (red) receives input from ipsilateral n.IX-X (green). Scale bars = 500 μm in A; 200 μm in B; 10 μm in C,D.

Reciprocal connections between DTAM and n.IX-X are also required for vocalization in terrestrial frogs. In *Rana pipiens*, calling was evoked in vivo by electrical stimulation of the ventral forebrain (Schmidt, 1968) or DTAM (Schmidt, 1974). In the denervated brain, bilateral lesions in DTAM eliminated neural correlates of electrically evoked vocal patterns recorded in n.IX-X, although inspiratory correlates remained (Schmidt, 1974). DTAM activity was correlated with fictive vocalizations (Schmidt, 1976), but DTAM could not independently generate these patterns. Damage to areas in or near n.IX-X eliminated normal neural correlates of vocal activity in DTAM (Schmidt, 1976, 1992), indicating that DTAM requires input from the caudal hindbrain to generate proper vocal patterns. Based on these findings, Schmidt (1992) proposed a model in which circuits in caudal n.IX-X produce respiratory patterns, whereas the network interactions between this region and DTAM are responsible for producing vocal patterns (modified respiratory activity).

In *Xenopus laevis*, en passant recordings from the laryngeal nerve of singing frogs reveal a pattern of compound action potentials matched one-to-one with the production of the click trains that make up different

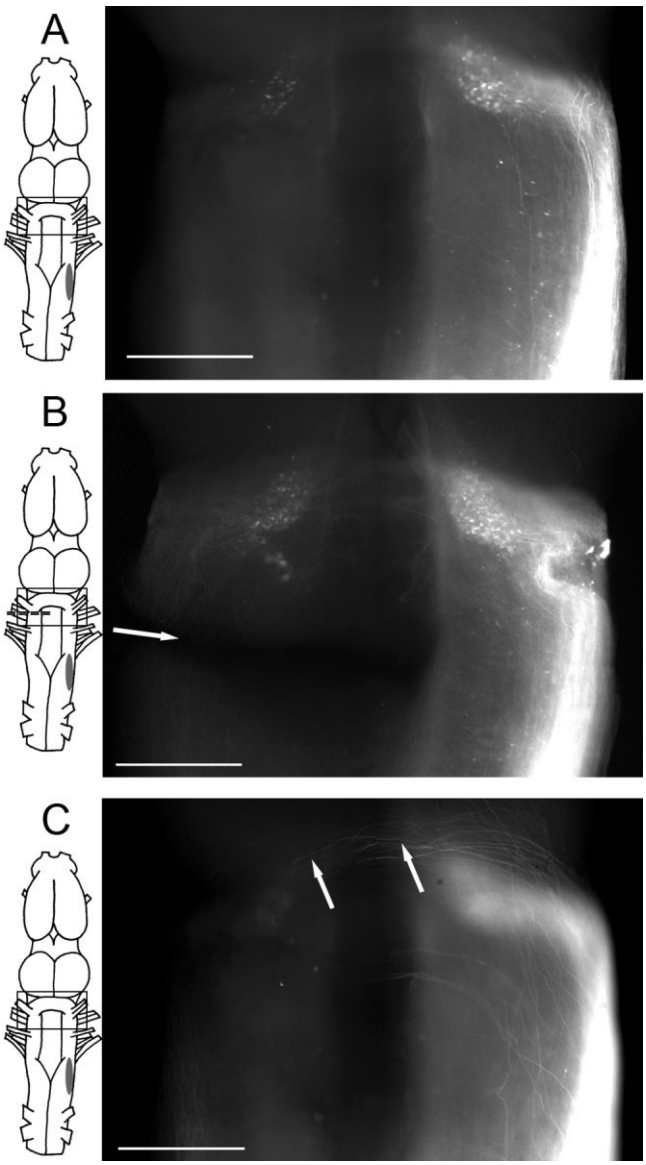

Fig. 9. Axon trajectories of $DTAM_{IX-X}$ neurons: n.IX-X injections. **A:** Dorsal view of a whole mount brain after n.IX-X injection reveals $DTAM_{IX-X}$ neurons in ipsilateral and contralateral nuclei. Anterior is up. **B:** $DTAM_{IX-X}$ neurons are labeled in comparable numbers following FR injection into n.IX-X in a brain transected through the contralateral tract (dashed line in diagram; arrow in photomicrograph). **C:** Contralateral $DTAM_{IX-X}$ projections seen in a whole-mount preparation. Axons descend ventrally and travel slightly anterior before crossing the midline and joining the descending axon tract (arrows). Scale bars = 500 μm.

Xenopus calls (Yamaguchi and Kelley, 2000). Thus, vocal patterns are produced in the brain. Whole-cell recordings reveal that laryngeal motor neurons require premotor inputs to produce vocal patterns (Yamaguchi et al., 2003). The anatomical projection from DTAM to laryngeal motor neurons implicates $DTAM_{IX-X}$ neurons as primary candidates for premotor input to the vocal circuit, as is also the case for terrestrial frogs.

Evolution of the neural network for vocalization: calling and breathing

The neural networks that drive vocal behaviors are believed to have evolved from more ancient networks that drive breathing rhythms (Bass and Baker, 1997). Vocal production in terrestrial frogs has been described in detail for *Rana pipiens*. Calling occurs during expiration and is produced by vibration of the vocal cords and pulsing of the glottal muscles (Schmidt, 1972). This vocal phase is followed by an inspiratory phase, during which air is returned to the lungs. In contrast, *Xenopus* do not breathe while producing sounds. Respiratory muscles are inactive during calling, whereas vocal muscles remain quiescent during breathing. Vocalizations are generated when paired discs of laryngeal arytenoid cartilage are rapidly separated by bilateral contraction of laryngeal dilator muscles (Yager, 1992). The larynx communicates with the lungs posteriorly and with the buccal cavity anteriorly via the glottis. The glottis remains closed during calling, while the frog is submerged, but is opened by glottal muscles when the frog rises to the surface to breathe. Both glottal and laryngeal muscles are innervated by axons that exit the brain in the fourth root of cranial nerve IX-X (Simpson et al., 1986). Thus, although *Xenopus* call without breathing, vocal and respiratory muscles are linked anatomically through a common nerve. These laryngeal (vocal) and glottal (respiratory) motor neurons also reside in a shared motor nucleus, n.IX-X, though they are topographically distinct. How are distinct laryngeal and glottal motor neuron activities produced?

DTAM projections to glottal motor neurons provide a potential substrate for gating activity during respiration. In *Rana pipiens*, in addition to robust DTAM activity during expiratory-gated calling, lower amplitude activity during the inspiratory phase was recorded by Schmidt (1976). This observation supports the possibility that DTAM might affect both the expiratory and the inspiratory phases of calling in terrestrial frogs. A similar role for DTAM in *Xenopus* is suggested by its projection to the pool of glottal motor neurons. However, in *Xenopus*, glottal opening should be inhibited during calling, because breathing does not occur. In terms of an evolutionary trajectory, one possibility is that an excitatory connection in a terrestrial ancestor has switched to become inhibitory (either directly or via an inhibitory interneuron) so that DTAM can silence glottal motor neuron activity while simultaneously activating laryngeal motor neurons. Because DTAM provides input to both glottal and laryngeal motor neurons, it may serve as a switch. For example, DTAM may activate vocal motor neurons in n.IX-X during calling and simultaneously provide an inhibitory signal to the glottal motor neurons.

Although *Xenopus* vocalization can proceed unpunctuated by breathing for many minutes, it is possible that networks that were responsible for generating respiratory patterns in terrestrial frog calls (and may still control breathing in *Xenopus*) have been co-opted by the vocal network to modulate calls in a periodic fashion, thus producing temporally modulated patterns of clicks. Alternatively, new networks dedicated solely to vocal production might have developed from the original respiratory circuit. Our finding of interspersed commissural neurons in n.IX-X with distinct projection patterns—anterior (glottal) or posterior (laryngeal)—may support the latter hypothe-

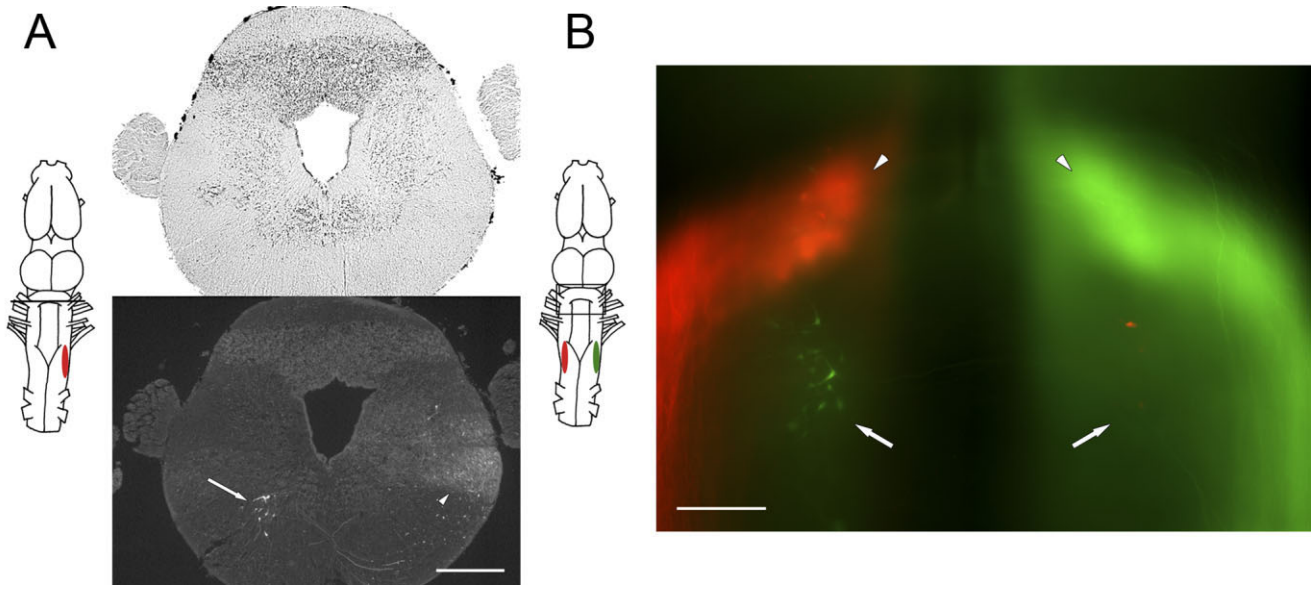

Fig. 10. Inputs to contralateral n.IX-X from the medial reticular formation: n.IX-X injections. **A:** Retrogradely labeled neurons (arrow) in the medial reticular formation (Rm) after injection into contralateral n.IX-X. Arrowhead illustrates fiber tract ascending toward DTAM. Dorsal is up. **B:** Dorsal view of a whole-mount brain following injection in left and right motor nuclei. Contralateral projection neurons in Rm (arrows) are ventral and caudal to DTAM (arrowheads). Anterior is up. Scale bars = 500 μm in A; 200 μm in B.

sis. In either case, the strong projection from n.IX-X to DTAM supports a model in which caudal and rostral hindbrain networks cooperate to generate vocal patterns. Now that we have identified several premotor neurons in the vocal circuit and know their projection trajectories and targets, we can test these hypotheses by using electrophysiological approaches.

Bilateral coordination of vocal networks

One requirement for proper song generation is simultaneous contraction of left and right laryngeal dilator muscles. Because muscle activity must be bilaterally synchronous, a group of cells connecting the motor nuclei is expected and indeed is found in other motor systems (Koshiya and Smith, 1999; Butt et al., 2002). DTAM is ideally suited to a role in coordinating bilateral motor output, because it projects bilaterally to n.IX-X. Unilateral DTAM stimulation in *Rana* produces bilaterally synchronized laryngeal nerve activity, whereas midline transections at the level of DTAM reduce bilateral coordination of fictive vocalizations (Schmidt, 1976). Our anatomical finding of strong bilateral projections from DTAM to n.IX-X (via an anterior hindbrain commissure at the level of DTAM) suggests that one role of DTAM in *Xenopus*, as in *Rana*, is to synchronize motor output.

Projections across the posterior commissure might also coordinate bilateral motor activity. Commissural neurons in n.IX-X connect the motor nuclei bilaterally, and neurons in n.IX-X project to contralateral DTAM. Axons of both projections cross the midline at the posterior commissure. In *Rana*, synchronization of inspiratory neural correlates remained after the brain was split at the level of DTAM but was lost after further splitting of the hindbrain more posteriorly (Schmidt, 1976). Thus, contralaterally projecting neurons might also contribute to the bilateral synchrony of n.IX-X motor output.

Role of the reticular formation

Two reticular formation networks (one anterior and one posterior) generate respiratory patterns in *Rana catesbeiana* (Wilson et al., 2002). The close association of Ri and n.IX-X neurons in *X. laevis* (Kelley et al., 1988) supports a possible role in respiratory and vocal pattern generation. Ipsilateral and contralateral Ri projections to DTAM further support the hypothesis that respiratory patterns generated in the posterior hindbrain are conveyed to DTAM, where they may be modified into proper vocal patterns. Ri axons projecting to contralateral DTAM first cross the midline, passing near n.IX-X before ascending to DTAM. Thus, although we observed labeled neurons in contralateral Ri following n.IX-X injection, we cannot distinguish whether Ri neurons project to contralateral Ri and n.IX-X or whether these cells are actually DTAM-projecting Ri neurons labeled via fibers of passage. Intracellular fills will be required to confirm the existence of commissural Ri neurons. A column of cells (~100 μm long) in contralateral medial reticular formation was observed following dextran injections into n.IX-X. Whether this newly identified neuronal population is, in fact, involved in respiratory or vocal production remains to be tested. In summary, we have identified neurons in the reticular formation that likely play a role in generating respiratory and vocal patterns, as well as coordinating rhythmogenesis bilaterally.

CONCLUSIONS

Similarities between *Xenopus* and *Rana* suggest that, despite evolutionary trajectories that diverged some 150 million years ago and the adoption of an entirely aquatic habitat by the pipids, elements of the hindbrain vocal network share many common features. These features include a prominent role for DTAM in generating vocal-

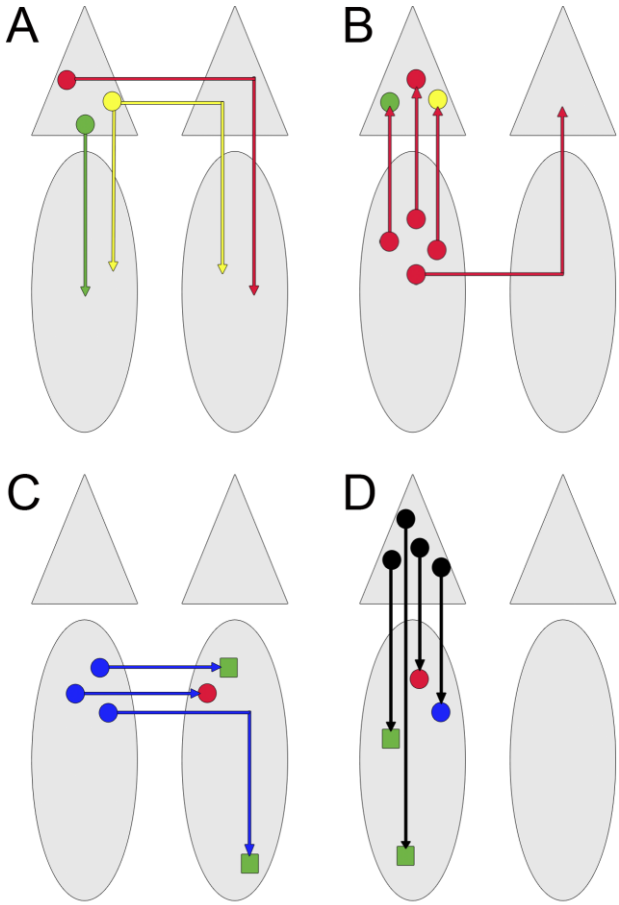

Fig. 11. Summary of vocal network connections. Schematics of *Xenopus* hindbrain vocal nuclei (triangles, DTAM; ovals, n.IX-X) are shown bilaterally in each panel. Circles represent projection neurons; squares represent motor neurons. **A:** $DTAM_{IX\text{-}X}$ neurons project to ipsilateral or contralateral n.IX-X or bilaterally. **B:** The three $DTAM_{IX\text{-}X}$ subtypes all receive ipsilateral input from $IX\text{-}X_{DTAM}$ neurons. $IX\text{-}X_{DTAM}$ cells also send some projections to contralateral DTAM. **C:** $IX\text{-}X_{IX\text{-}X}$ neurons project to anterior or posterior n.IX-X and target glottal and laryngeal motor neurons and $IX\text{-}X_{DTAM}$ neurons. **D:** $DTAM_{IX\text{-}X}$ cells project to four cell types identified in n.IX-X: glottal and laryngeal motor neurons, $IX\text{-}X_{IX\text{-}X}$ neurons, and $IX\text{-}X_{DTAM}$ neurons.

izations and coordinating bilateral motor activity, strong reciprocal connectivity between DTAM and n.IX-X, and the importance of reciprocal connections between left and right n.IX-X. Despite this apparent conservation, unique vocal production mechanisms in *Xenopus* require respiratory and vocal muscles to operate independently. We have identified connections in the vocal hindbrain network, including direct projections from DTAM to vocal and respiratory motor neurons, which may underlie this novel aquatic behavior.

ACKNOWLEDGMENTS

We thank Taffeta Elliott, Madeleine Johnson, Elizabeth Leininger, Martha Tobias, Clementine Vignal, and Eun-Jin Yang for helpful comments on the manuscript.

LITERATURE CITED

Bass AH, Baker R. 1997. Phenotypic specification of hindbrain rhombomeres and the origins of rhythmic circuits in vertebrates. Brain Behav Evol 50(Suppl 1):3–16.

Brahic CJ, Kelley DB. 2003. Vocal circuitry in *Xenopus laevis*: telencephalon to laryngeal motor neurons. J Comp Neurol 464:115–130.

Butt SJB, Harris-Warrick RM, Kiehn O. 2002. Firing properties of identified interneuron populations in the mammalian hindlimb central pattern generator. J Neurosci 22:9961–9971.

Evans BJ, Kelley DB, Tinsley RC, Melnick DJ, Cannatella DC. 2004. A mitochondrial DNA phylogeny of African clawed frogs: phylogeography and implications for polyploidy evolution. Mol Phylogenet Evol 33:197–213.

Kelley DB. 1980. Auditory and vocal nuclei in the frog brain concentrate sex hormones. Science 207:553–555.

Kelley DB, Fenstemaker S, Hannigan P, Shih S. 1988. Sex differences in the motor nucleus of cranial nerve IX-X in *Xenopus laevis*: a quantitative Golgi study. J Neurobiol 19:413–429.

Koshiya N, Smith JC. 1999. Neuronal pacemaker for breathing visualized in vitro. Nature 400:360–363.

Luksch H, Walkowiak W, Muñoz A, ten Donkelaar HJ. 1996. The use of in vitro preparations of the isolated amphibian central nervous system in neuroanatomy and electrophysiology. J Neurosci Methods 70:91–102.

Martin WF, Gans C. 1972. Muscular control of the vocal tract during release signaling in the toad *Bufo valliceps*. J Morphol 137:1–28.

Schmidt RS. 1968. Preoptic activation of frog mating behavior. Behaviour 30:239–257.

Schmidt RS. 1972. Action of intrinsic laryngeal muscles during release calling in leopard frog. J Exp Zool 181:233–244.

Schmidt RS. 1974. Neural correlates of frog calling: trigeminal tegmentum. J Comp Physiol 92:229–254.

Schmidt RS. 1976. Neural correlates of frog calling: isolated brainstem. J Comp Physiol 108:99–113.

Schmidt RS. 1992. Neural correlates of frog calling: production by two semi-independent generators. Behav Brain Res 50:17–30.

Shaw BK, Kelley DB. 2005. Dissecting vocal pattern production in *Xenopus* with interspecies chimeras. Soc Neurosci Abstr 1001:5.

Simpson HB, Tobias ML, Kelley DB. 1986. Origin and identification of fibers in the cranial nerve IX-X complex of *Xenopus laevis*: Lucifer yellow backfills in vitro. J Comp Neurol 244:430–444.

Tobias ML, Kelley DB. 1987. Vocalizations by a sexually dimorphic isolated larynx: peripheral constraints on behavioral expression. J Neurosci 7:3191–3197.

Tobias ML, Viswanathan SS, Kelley DB. 1998. Rapping, a female receptive call, initiates male–female duets in the South African clawed frog. Proc Natl Acad Sci U S A 94:1870–1875.

Tobias ML, Barnard C, O'Hagan R, Horng SH, Rand M, Kelley DB. 2004. Vocal communication between male *Xenopus laevis*. Anim Behav 67: 353–365.

Weinberg RJ, van Eyck SL. 1991. A tetramethybenzidine/tungstate reaction for horseradish peroxidase histochemistry. J Histochem Cytochem 39:1143–1148.

Wetzel DM, Kelley DB. 1983. Androgen and gonadotropin effects on male mate calls in South African clawed frogs, *Xenopus laevis*. Horm Behav 17:388–404.

Wetzel DM, Haerter UL, Kelley DB. 1985. A proposed neural pathway for vocalization in South African clawed frogs, *Xenopus laevis*. J Comp Physiol A157:749–761.

Wilson RJA, Vasilakos K, Harris MB, Straus C, Remmers JE. 2002. Evidence that ventilatory rhythmogenesis in the frog involves two distinct neuronal oscillators. J Physiol 540:557–570.

Yager D. 1992. A unique sound production mechanism in the pipid anuran *Xenopus borealis*. Zool J Linn Soc 104:351–375.

Yamaguchi A, Kelley DB. 2000. Generating sexually differentiated vocal patterns: laryngeal nerve and EMG recordings from vocalizing male and female African clawed frogs (*Xenopus laevis*). J Neurosci 20:1559–1567.

Yamaguchi A, Kaczmarek LK, Kelley DB. 2003. Functional specialization of male and female vocal motoneurons. J Neurosci 23:11568–11576.